FEBS 18343 FEBS Letters 405 (1997) 299–304

Ion channels formed by HIV-1 Vpu: a modelling and simulation study

A.L. Grice, I.D. Kerr, M.S.P. Sansom*

Laboratory of Molecular Biophysics, The Rex Richards Building, University of Oxford, South Parks Road, Oxford OX1 3QU, UK

Received 21 January 1997

Abstract Vpu is an oligomeric integral membrane protein encoded by HIV-1 which forms ion channels, each subunit of which contains a single transmembrane helix. Models of Vpu channels formed by bundles of $N=4$, 5 or 6 transmembrane helices have been developed by restrained molecular dynamics and refined by 100 ps simulations with water molecules within the pore. Pore radius profiles and conductance predictions suggest that the $N=5$ model corresponds to the predominant channel conductance level of the channel. Potential energy profiles for translation of Na^+ or Cl^- ions along the Vpu $N=5$ pore are consistent with the weak cation selectivity of Vpu channels.

Key words: HIV-1; Vpu; Ion channel; Molecular dynamics; Conductance

1. Introduction

Vpu is an integral membrane protein encoded by HIV-1 [1]. It is 80–82 residues long (depending on the viral isolate) and contains a single transmembrane helix from residue 6 to 28. It is present in the Golgi and endoplasmic reticulum membranes of infected cells and is believed to form oligomers within those membranes. The C-terminal cytoplasmic domain of Vpu has been shown by NMR to adopt a helix-loop-helix-turn conformation [2]. The loop between the two helices contains serine residues 52 and 57, which can be phosphorylated in vivo [3]. Vpu has two biological roles, which appear to correspond to the two distinct domains within the protein [4]. The C-terminal cytoplasmic domain is associated with induction of CD4 degradation in the endoplasmic reticulum. The N-terminal transmembrane domain is concerned with control of virus release/secretion from HIV-1 infected cells.

For some time it has been suggested that Vpu may act as an ion channel [5]. The suggestion arose by analogy with the M2 protein from influenza A [6], which forms proton activated and permeable channels, and which, although it does not share any sequence homology with Vpu, exhibits a similar transmembrane topology. Two studies provide evidence in support of Vpu forming ion channels. Expression of Vpu in *E. coli* cells produced protein which, when purified and incorporated into planar lipid bilayers, resulted in channel formation [7]. The channels had conductances ranging from 15 to 280 pS, and were weakly (about 5×) selective for Na^+ over Cl^- ions. Furthermore, expression of Vpu in *E. coli* resulted in an increase in the Na^+ permeability of the bacterial cell membrane. Further evidence is provided by expression of Vpu in frog oocytes [8] which results in a cation selective conductance. If a mutant Vpu, in which the sequence of the TM segment of Vpu was 'scrambled', was expressed in oocytes a cation selective conductance was not induced. Furthermore, the 'scrambled' TM Vpu did *not* promote virus release. A synthetic peptide corresponding to the TM segment of Vpu formed channels in planar lipid bilayers, ranging in conductance from 10 to 60 pS. The corresponding 'scrambled' TM peptide failed to form discrete channels in lipid bilayers. Overall, these data support the proposal that Vpu is a channel protein, and suggest that the N-terminal TM domain is largely responsible for channel formation and for promotion of virus release.

How may a membrane protein containing a single TM segment form an ion channel? The most likely mechanism is via the TM segment adopting an α-helical conformation, and an oligomer of approximately parallel TM helices associating within a bilayer to surround a central pore. The dimensions of the pore, and hence its conductance, would depend upon the oligomeric state, i.e. the N number of helices/bundle. Ion channel formation by bundles of TM α-helices has been discussed for a number of different systems [9–11]. For example, the antibiotic peptide alamethicin [12] has been shown experimentally to be α-helical, and to form parallel helix bundles which form ion channels in bilayers. These channels exhibit multiple conductance levels, with the higher conductance levels corresponding to a larger number of α-helices in the channel assembly. The influenza M2 protein is the best studied ion channel encoded by a virus [6]. It forms channels activated by a lowered pH which are proton selective [13]. M2 contains a single TM segment, and forms tetramers within the membrane. A synthetic peptide corresponding to the TM domain has been shown to form ion channels in planar lipid bilayers [14], and to adopt an α-helical conformation [15]. Thus in many ways the influenza A M2 protein is a paradigm for channel formation by viral proteins containing a single TM helix.

It is possible to generate plausible molecular models of ion channels formed by parallel bundles of TM helices [16]. This approach has been used to explore channel formation by a number of proteins, including influenza A M2 [17,18]. Such models may form the basis of approximate calculations of channel conductance [19,20] and of ion selectivity [21]. In this paper we present models for the different conductance states of Vpu channels, and relate the predicted properties of these models to the experimental data.

2. Materials and methods

2.1. General

Model building was performed using Xplor V3.1 [22] with the CHARMm PARAM19 [23] parameter set. Only those H atoms attached to polar groups were represented explicitly; apolar groups were represented using extended carbon atoms. Visualisation of models was carried out using Quanta V4.1 (Biosym/Molecular Simulations), and diagrams of structures were drawn using Quanta and Mol-

*Corresponding author. Fax: (44) (1865) 275182.
E-mail: mark@biop.ox.ac.uk

PII S0014-5793(97)00198-1

script [24]. MD simulations on the solvated models were performed using CHARMm [23] version 23f3. Simulations were run on a DEC 2100 4/275. All other calculations were on Silicon Graphics workstations.

2.2. In vacuo modelling

Initial models of the channels were generated by restrained molecular dynamics (MD) simulations, performed in vacuo, and using a simulated annealing protocol as described in [16].

2.3. MD simulations of solvated pore models

Solvation of selected (see below) in vacuo models followed by extended MD simulations were carried out as described [25]. Model pores were solvated in Quanta using pre-equilibrated boxes of water molecules. Water molecules were selected such that the central pore and the cap regions at either mouth of the pore were solvated, but such that no water molecules were present on the bilayer-exposed faces of the pores. The water model employed was a TIP3P three-site model [26] with partial charges $q_O = -0.834$ and $q_H = +0.417$. During these simulations restraints were applied: to prevent evaporation of water molecules from the mouths of the pore; to maintain the TM segments in an α-helical conformation; and to hold together the helix bundle [18,21]. Additionally, a bilayer potential based on residue-by-residue hydrophobicities [27], was employed to mimic the embedding of the helix bundle in a membrane. MD simulations employed a 1 fs timestep. The production stage of the simulation was for 85 ps, giving a total simulation time of 100 ps. Trajectories were analysed using coordinate sets saved every 1 ps during the production stage of the simulations. Non-bonded interactions (both electrostatic and van der Waals) between distant atoms were truncated using a shift function with a cutoff of 13.0 Å, and a fixed dielectric of $\varepsilon = 1$ was used for electrostatic interactions.

2.4. MD simulations with an ion in the pore

Short MD simulations with an ion restrained to lie in successive *xy*-planes along the pore (*z*) axis were performed. For step *i* the ion was placed at $(0,0,z_i)$ and subjected to a quadratic planar restraint with a force constant of 10 kcal/mol/Å^2. At each step the system was subjected to 1000 steps of ABNR energy minimisation (to relax any bad contacts between water and ion) followed by 6 ps heating and 9 ps equilibration MD. This process was repeated for the ion at $z_i = -15$ to +15 Å, in 1 Å steps. Potential energies of interaction energies of the ion with the pore and/or water were calculated as: (i) ΔE(ion/pore+water) = E(pore+water+ion) − E(pore+water) − E(ion); (ii) ΔE(ion/pore) = E(pore+ion) − E(pore) − E(ion); and ΔE(ion/water) = E(water+ion) − E(water) − E(ion).

3. Results

3.1. Generation of in vacuo models

Initial models of pores were generated by in vacuo restrained MD simulations. It is important to make explicit the assumptions which are embodied in these models. The sequence of the TM segment used (see Fig. 1A) was the same as that described in [7], and was based on comparison of Vpu sequences from different HIV-1 isolates alongside prediction of TM helix positions using the program MEMSAT [28]. The resultant TM segment (residues 6–28) has a high frequency of β-branched amino acids (i.e. Val and Ile). It has been shown (e.g. [29]) that such residues have a high propensity for α-helix formation in a lipid bilayer environment, thus justifying the assumption that the TM segment forms an α-helix. The third assumption is that the α-helices of the bundle are approximately parallel. This is justified on the basis that all the Vpu chains are inserted into the bilayer in the same orientation, i.e. with the C-terminal domain cytoplasmic. Channels were modelled as bundles of $N = 4$, 5 or 6 helices/bundle. Crude calculations of the conductances expected for different values of N [11,12] suggest that $N = 3$ bundles would have a pore too narrow to support permeation of ions, and that $N > 6$ would form pores of higher conductance than those which have been observed experimentally. The final assumption concerns the orientation of the α-helices within the bundle by rotation about their long axes. The Vpu TM sequence contains a single polar residue, Ser-24. On energetic grounds one would expect this residue to be directed towards the lumen of the pore, rather than towards the surrounding lipid. Furthermore, there is considerable experimental evidence for e.g. the nicotinic acetylcholine receptor [30] for Ser residues forming the pore lining of cation selective

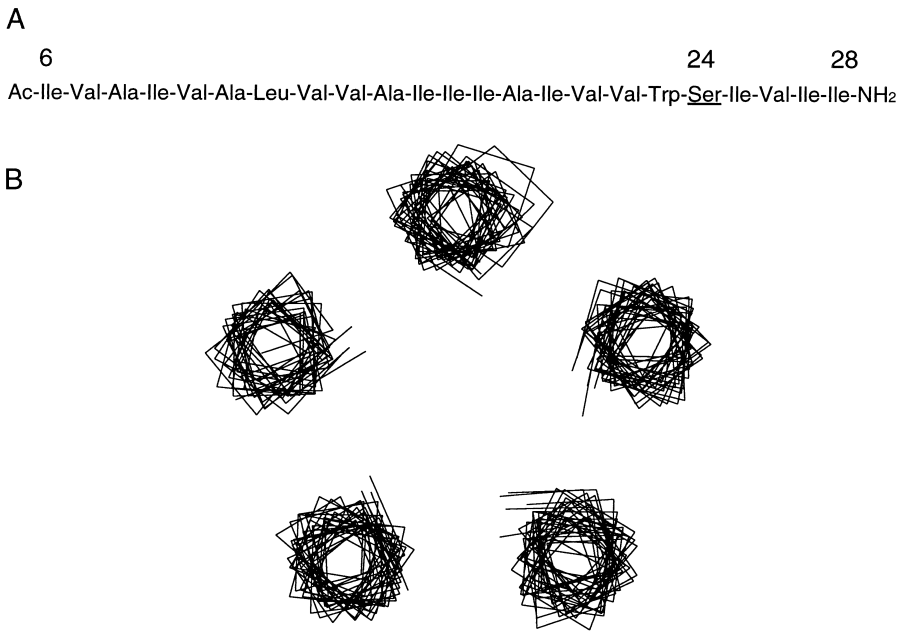

Fig. 1. Generation of in vacuo models from the Vpu TM sequence. A: Sequence of the Tm segment, with the pore-lining Ser-24 residue highlighted. B: Cα traces five $N = 5$ structures superimposed.

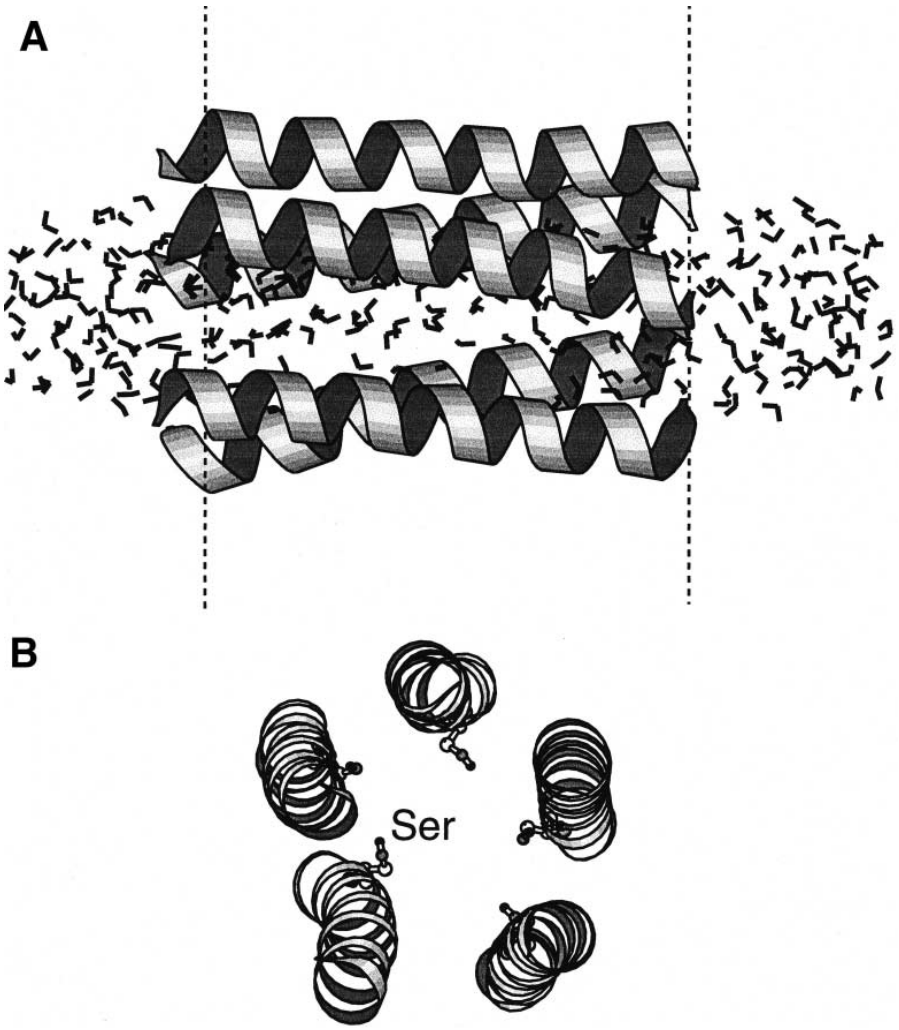

Fig. 2. Diagrams of the solvated $N=5$ model, drawn using Molscript [24]. A: View perpendicular to the pore (z) axis, with the N-termini on the left-hand side, showing the helices as ribbons and water molecules in 'bonds' format. Dotted lines at $z=\pm 15.75$ Å indicate the limits of the bilayer potential used during the MD simulations. B: View down the z axis, showing the ring of Ser-24 residues in 'ball-and-stick' format.

channels. Thus, the Vpu TM helices were oriented such that their Ser-24 residues were directed towards the centre of the helix bundle.

These assumptions were embodied in Cα templates, i.e. idealised models of the pores containing only the Cα atoms [16]. These models were used as input to in vacuo restrained MD, to generate an ensemble of 25 structures for each model (i.e. for $N=4$, 5 and 6). Within a given ensemble there is a degree of structural variation (Fig. 1B). Simple statistical analysis of an ensemble may be used to describe geometrical properties common to the helix bundles of all structures. In particular, examination of the three Vpu ensembles revealed mean helix crossing angles [31] of -3.6 (± 3.7)°, $+1.2$ (± 3.1)° and $+1.0$ (± 4.4)° for $N=4$, 5 and 6 respectively. Such helix crossing angles correspond to helix bundles without any appreciable degree of supercoiling, which differs from what has been observed in other systems [16] but which may correlate with the high frequency of β-branched sidechains. Visual inspection of the models revealed that, apart from Ser-24 (see below), the non-β-branched sidechains all clustered on the external lipid-exposed face of the bundle, and thus the helix-helix interfaces were made up entirely of contacts between β-branched sidechains. Mean helix-to-helix separations were 9.6 (± 0.2) Å, 9.5 (± 0.2) Å and 9.6 (± 0.2) Å for $N=4$, 5 and 6 respectively, indicative of close packing of the helices.

3.2. *Refinement of models by MD simulations in the presence of pore water molecules*

The in vacuo procedure produced likely initial models of pores formed by parallel bundles of Vpu helices. These were refined by 100 ps MD simulations with explicit water molecules present within either mouth of the channels. One structure was selected from each ensemble for such refinement. As most channels are believed to exhibit rotational symmetry about the central axis [32], the structure with the greatest degree of rotational symmetry was selected. During these MD simulations an empirical hydrophobicity potential was applied to the amino acid sidechains in order to mimic the presence of the lipid bilayer.

As anticipated there were dynamic fluctuations in helix packing during the course of the MD simulations. Averaging over the duration of the simulations, the mean helix crossing angles were -8.7 (± 1.9)°, -6.6 (± 9.6)° and $+10.0$ (± 8.2)° for $N=4$, 5 and 6 respectively. This suggested a degree of left-handed supercoiling in the $N=4$ bundle, whereas in the two higher order bundles there is no clear evidence of supercoiling

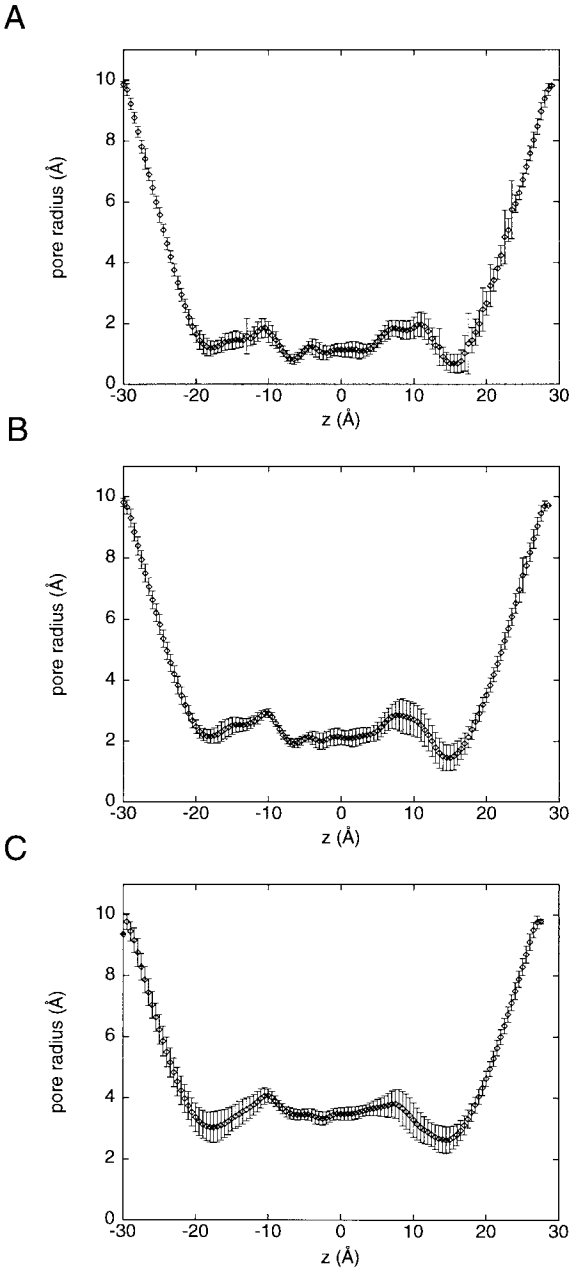

Fig. 3. Pore radius profiles for the (A) $N=4$, (B) $N=5$, and (C) $N=6$ solvated models. Each profile is an average (±S.D.) taken across the MD trajectory. The N-terminal mouth of the pore is ca. $z=-18$ Å; the C-terminal mouth is ca. $z=+18$Å.

over and above the dynamic fluctuations in helix packing. Mean helix-to-helix separations were 10.2 (±0.3) Å, 10.7 (±0.4) Å and 10.4 (±0.5) Å for $N=4$, 5 and 6 respectively. Thus, there is a limited degree of expansion of the helix bundles upon solvation, as has been observed for simulations on other, comparable systems [25] Fig. 2.

To characterise the nature of the pore lining it is of interest to determine the conformations of the Ser-24 sidechains [33] which line the pore. These were analysed in terms of the χ_1 and χ_2 torsion angles of the Ser residues during the MD trajectories. Throughout the trajectories of all three bundles ($N=4$, 5 and 6) the value of χ_1 (which positions the Oγ atom) was ca. −60°, characteristic of a *g*+ conformation. The value of χ_2 (which positions the Hγ atom) switched between −60° and +60°. Overall, the conformation $(\chi_1, \chi_2)=(-60°, +60°)$ was the most heavily populated. This corresponds to the Ser sidechain forming an H-bond back to the carbonyl oxygen of the main chain of the preceding turn of the α-helix [34]. Consequently, the ring of Ser-24 sidechains presents a ring of hydroxyl oxygen lone pair electrons to the lumen of the pore (see below).

The dynamic behaviour of the water molecules during these simulations was also examined. As in previous simulations of pores formed by helix bundles [25], water molecules within the pore exhibited reduced translational and rotational mobility relative to bulk water and to water molecules present at either mouth of the pore. This was most pronounced for the $N=4$ bundle, the water molecules within which had self-diffusion and rotational reorientation rates almost an order of magnitude lower than those of bulk water. Also in common with previous simulations [25], the waters within the pore were aligned such that, on average, their dipoles are anti-parallel to the α-helix dipoles.

3.3. Prediction of channel properties

The MD refined models were used to predict channel properties for Vpu helix bundles with different N values. Using the program HOLE [35] pore radius profiles (i.e. variation in pore radius along the length of the pore) were evaluated (Fig. 3). As expected the pore radius increases with the number of helices in the bundle (Table 1). For the $N=4$ and 5 bundles there is a constriction of the pore at the C-terminal mouth, which is less pronounced for the $N=6$ bundle. Pore radius profiles may be used to predict single channel conductances. This is based upon a simple Ohmic calculation of the conductance of an irregular 'tube' of electrolyte solution of the same dimensions as the interior of the channel [19,20]. It has been shown that such a calculation yields an estimate of the channel conductance which is ca. 5 times too high for a number of channels of known structure [20]. Thus, scaling of the calculated Ohmic conductance by a factor of 0.2× yields a prediction of the conductance (Table 1). From this it can be seen that the $N=5$ helix bundle is predicted to have a conductance of ca. 60 pS. This correlates well with single channel conductances observed in [8], suggesting that the $N=5$ bundle may correspond to a major channel species.

3.4. Potential energy profiles

Potential energy profiles were calculated corresponding to translation of a Na^+ and of a Cl^- ion along the $N=5$ pore, in the presence of water molecules. This yields a first approximation to the energetics of interaction of these ions with the model pore, although it must be stressed that it does *not* yield a free energy profile. The resultant potential energies may be used to construct interaction energy profiles (Fig. 4). The Na^+ interaction energy profiles (Fig. 4A) reveal a markedly favour-

Table 1
Properties of solvated pore models

N	No. of waters	Minimum pore radius (Å)	Predicted conductance (pS)
4	139	ca. 0.7	21
5	257	ca. 1.5	57
6	381	ca. 2.5	93

Conductance predictions, made using the method of [20], refer to 500 mM NaCl as the electrolyte solution.

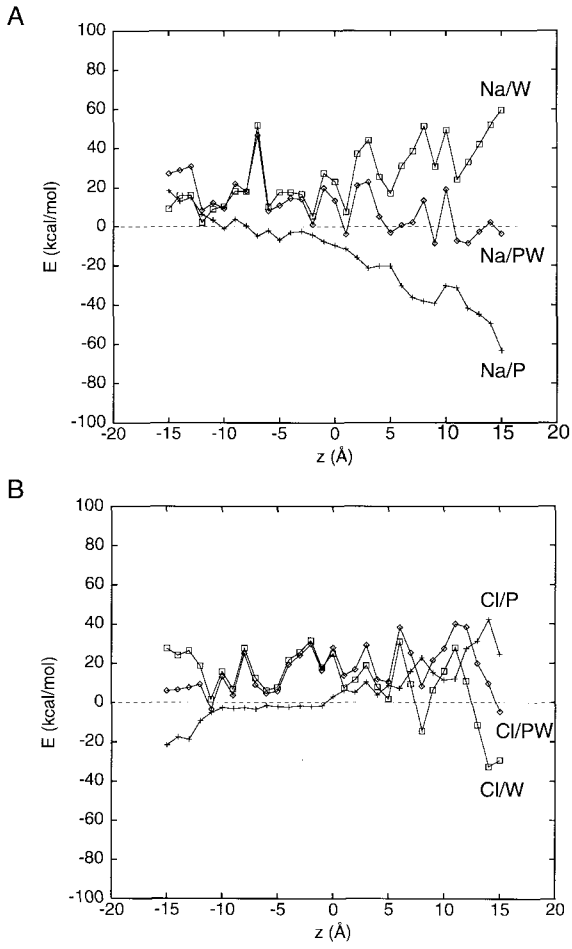

Fig. 4. Potential energy profiles for ion/channel interactions for the $N=5$ model. A: Energy profiles for an Na^+ ion; B: energy profiles for a Cl^- ion. In each case the three lines correspond to the: ◇ ion/(pore+water); + ion/pore; and □ ion/water interaction energies. The ion/(pore+water) and ion/water interaction energies have been normalized by subtraction of the mean potential energy of the corresponding ion simulated in a box of 3375 water molecules.

able component to the ion/protein interaction energy at the C-terminal mouth, presumably corresponding to the ring of Ser-24 oxygens directed towards the lumen of the pore. This is to some extent counteracted by a less favourable Na^+/water interaction energy in this region, such that the overall ion/(pore+water) profile is rather flat. In contrast, the Cl^-/protein energy profile (Fig. 4B) shows an unfavourable interaction in this region. The overall energy profile for Cl^- is also rather flat, but is slightly less favourable than for Na^+, which parallels the observed weak cation selectivity of the channel.

4. Discussion

4.1. Critique of models

It is important to consider the limitations of the modelling and simulation methods employed in this study. A major problem is the absence of any substantial protein chemistry or structural data for the TM region of Vpu. However, in the light of the evidence for the oligomeric nature of Vpu [1] and by analogy better characterised systems e.g. influenza M2, the assumptions underlying modelling the Vpu channel as a bundle of approximately parallel helices seem justified. We have a degree of confidence in the computational methodology per se as it has already been employed to model a number of channels formed by α-helix bundles [16,33,36,37].

An explicit bilayer was not included in the simulations, as this would lead to a considerable increase in cpu time. However, as the direct interactions of the water molecules are with one another and with the protein atoms lining the pore, omission of a lipid bilayer is an acceptable first approximation. The other major omission from the model is the C-terminal cytoplasmic domain [2]. As a first approximation this is not too serious, as the synthetic Vpu TM helices have been shown to self-assemble in a lipid bilayer to form channels [8] which resemble those of the intact protein [7]. However, it will clearly be essential in the future to extend the MD simulations to a more complete model of the channel which includes the C-terminal domain, and which is embedded in an explicit bilayer.

4.2. Comparison with experimental data

A major assumption underlying these models for which there is no direct experimental support is the number of helices which self-assemble to form a Vpu channel. Comparison of predicted conductances with those observed experimentally allows one to make an estimate of N. The conductances for channels formed by the synthetic peptide [8] range from 12 to 48 pS in 0.5 M NaCl. Similarly, in 0.5 M KCl a major conductance level of 61 pS is observed, which if normalised using bulk electrolyte conductivities is equivalent to 49 pS in 0.5 M NaCl. The predicted conductance of the $N=5$ pore is 57 pS in 0.5 M NaCl. This is a good level of agreement given the expected accuracy of such predictions [20], suggesting that the ca. 50 pS conductance observed experimentally corresponds to a pentameric assembly of Vpu TM helices. The lower conductance levels are therefore predicted to correspond to $N=4$ bundles. Measurements on the intact protein [7] yielded conductances from 15 to 280 pS. Whilst the lower value is comparable to that predicted for a tetrameric assembly, the upper value suggests that assemblies with $N>6$ may be formed, at least in vitro. Overall, the most likely channel assembly is a pentamer, but higher and lower N assemblies may also be formed. Definitive single channel data on Vpu channels in vivo would help to resolve this question, as would improved conductance prediction methods.

Both macroscopic current [8] and single channel [7] data suggest that Vpu channels are weakly selective for cations over anions. This is consistent with the calculated ion interaction energy profiles. However, it must be stressed that the simulations on which these profiles are based are relatively crude. A better picture of ion selectivity would be obtained by performing more extensive simulations to yield free energy profiles [38]. However, before conducting these, extension of the models (see above) is required. For example, immediately C-terminal to the Vpu TM helix is a cluster of charged residues, which may contribute to the selectivity filter of the channel. Modelling the conformation of these will require careful consideration of how they may interact with adjacent lipid headgroups. It would seem that a better understanding of the Vpu channel will require further electrophysiological and protein chemical data, alongside more detailed simulations.

Acknowledgements: This work was supported by a grant from the Wellcome Trust. Our thanks to Gary Ewart and Peter Gage (JCSMR,

ANU, Canberra) for their interest in this work, and to the Oxford Centre for Molecular Sciences for the use of computational facilities.

References

[1] Maldarelli, F., Chen, M.Y., Willey, R.L. and Strebel, K. (1993) J. Virol. 67, 5056–5061.
[2] Federau, T., Schubert, U., Flossdorf, J,. Henklein, P., Schomburg, D. and Wray, V. (1996) Int. J. Pept. Prot. Res. 47, 297–310.
[3] Henklein, P., Schubert, U., Kunert, O., Klabunde, S., Wray, V., Kloppel, K.D., Kiess, M., Porstmann, T. and Schomberg, D. (1993) Peptide Res. 6, 79–87.
[4] Schubert, U., Bour, S., Ferrer-Montiel, A.V., Montal, M., Maldarelli, F. and Strebel, K. (1996) J. Virol. 70, 809–819.
[5] Schubert, U., Henklein, P., Bour, S., Ferrer-Montiel, A.V., Oblatt-Montal, M., Montal, M. and Strebel, K. (1995) AIDS Res. Human Retrov. 11, S114.
[6] Holsinger, L.J., Nichani, D., Pinto, L.H. and Lamb, R.A. (1994) J. Virol. 68, 1551–1563.
[7] Ewart, G.D., Sutherland, T., Gage, P.W. and Cox, G.B. (1996) J. Virol. 70, 7108–7115.
[8] Schubert, U., Ferrer-Montiel, A.V., Oblatt-Montal, M., Henklein, P., Strebel, K. and Montal, M. (1996) FEBS Lett. 398, 12–18.
[9] Oiki, S., Madison, V. and Montal, M. (1990) Proteins Struct. Funct. Genet. 8, 226–236.
[10] Sansom, M.S.P., Kerr, I.D. and Mellor, I.R. (1991) Eur. Biophys. J. 20, 229–240.
[11] Sansom, M.S.P. (1991) Prog. Biophys. Mol. Biol. 55, 139–236.
[12] Sansom, M.S.P. (1993) Q. Rev. Biophys. 26, 365–421.
[13] Chizhmakov, I.V., Geraghty, F.M., Ogden, D.C., Hayhurst, A., Antoniou, M. and Hay, A.J. (1996) J. Physiol. 494, 329–336.
[14] Duff, K.C. and Ashley, R.H. (1992) Virology 190, 485–489.
[15] Duff, K.C., Kelly, S.M., Price, N.C. and Bradshaw, J.P. (1992) FEBS Lett. 311, 256–258.
[16] Kerr, I.D., Sankararamakrishnan, R., Smart, O.S. and Sansom, M.S.P. (1994) Biophys. J. 67, 1501–1515.
[17] Sansom, M.S.P. and Kerr, I.D. (1993) Prot. Eng. 6, 65–74.
[18] Sansom, M.S.P. Kerr, I.D., Smith, G.R. and Son, H.S. (1997) Virology (submitted).
[19] Sansom, M.S.P. and Kerr, I.D. (1995) Biophys. J. 69, 1334–1343.
[20] Smart, O.S., Breed, J., Smith, G.R. and Sansom, M.S.P. (1997) Biophys. J. 25, 139–150.
[21] Sansom, M.S.P., Smith, G.R., Smart, O.S. and Smith, S.O. (1997) Prot. Eng. (in press).
[22] Brünger, A.T. (1992) in Yale University Press, New Haven, CT.
[23] Brooks, B.R., Bruccoleri, R.E., Olafson, B.D., States, D.J., Swaminathan, S. and Karplus, M. (1983) J. Comp. Chem. 4, 187–217.
[24] Kraulis, P.J. (1991) J. Appl. Crystallogr. 24, 946–950.
[25] Breed, J., Sankararamakrishnan, R., Kerr, I.D. and Sansom, M.S.P. (1996) Biophys. J. 70, 1643–1661.
[26] Jorgensen, W.L., Chandresekhar, J., Madura, J.D., Impey, R.W. and Klein, M.L. (1983) J. Chem. Phys. 79, 926–935.
[27] Biggin, P.C. and Sansom, M.S.P. (1996) Biophys. Chem. 60, 99–110.
[28] Taylor, W.R., Jones, D.T. and Green, N.M. (1994) Proteins Struct. Funct. Genet. 18, 281–294.
[29] Deber, C.M. and Goto, N.K. (1996) Nature Struct. Biol. 3, 815–818.
[30] Sankararamakrishnan, R., Adcock, C. and Sansom, M.S.P. (1996) Biophys. J. 71, 1659–1671.
[31] Chothia, C., Levitt, M. and Richardson, D. (1981) J. Mol. Biol. 145, 215–250.
[32] Unwin, N. (1989) Neuron 3, 665–676.
[33] Mitton, P. and Sansom, M.S.P. (1996) Eur. Biophys. J. (in press).
[34] Gray, T.M. and Matthews, B.M. (1984) J. Mol. Biol. 175, 75–81.
[35] Smart, O.S., Goodfellow, J.M. and Wallace, B.A. (1993) Biophys. J. 65, 2455–2460.
[36] Kerr, I.D., Doak, D.G., Sankararamakrishnan, R., Breed, J. and Sansom, M.S.P. (1996) Prot. Eng. 9, 161–171.
[37] Breed, J., Biggin, P.C., Kerr, I.D., Smart, O.S. and Sansom, M.S.P. (1997) Biochim. Biophys. Acta (in press).
[38] Roux, B. and Karplus, M. (1991) Biophys. J. 59, 961–981.